

1 Is within-host viral community assembly shaped by local adaptation?

2

3 Maija Jokinen¹, Hanna Susi^{1,2} & Anna-Liisa Laine¹

4 ¹ Department of Organismal and Evolutionary Biology, Faculty of Biological and
5 Environmental Sciences, PO BOX 65, 00014, University of Helsinki, Finland

6 ² Department of Agricultural Sciences, Faculty of Agriculture and Forestry, PO BOX 27,
7 00014, University of Helsinki, Finland

8

9 Corresponding author: Maija Jokinen maija.jokinen@helsinki.fi

10 Running title: Viral local adaptation

11 local adaptation, coevolution, viruses, host-parasite coevolution

12

13

14

15

16

17

18 Abstract

19 Host-parasite coevolution describes the continuous reciprocal selection driving host defense
20 and parasite infectivity, with direct consequences for disease dynamics. While abundant
21 evidence exists for coevolution shaping host-parasite dynamics within the ‘one host-one
22 parasite’ framework, hosts are typically infected by multiple parasites and the extent to which
23 coevolutionary processes shape within-host parasite communities remains poorly understood.
24 Investigating these interactions is essential for understanding how coevolution drives parasite
25 diversity, competition, and coexistence within hosts. Here, we conducted a local adaptation
26 experiment to investigate the effects of coevolution on within-host viral community assembly
27 in *Plantago lanceolata*. Greenhouse-grown individuals were reciprocally transplanted into
28 wild populations during natural viral epidemics. We combined small-RNA sequencing to
29 identify the viral communities and joint species distribution modelling to quantify the effects
30 of local adaptation, population and host characteristics on viral community assembly. Our
31 results show that host populations vary in the extent to which local adaptation influences
32 within-host viral diversity. Across all populations, host maternal line and origin population
33 were the main determinants of viral community composition and infection status. The effects
34 varied across virus families, suggesting virus-specific assembly processes and variation in the
35 potential for coevolution to shape these interactions.

36
37

38

39

40

41

42 Introduction

43 Coevolutionary theory predicts reciprocal selection to drive key interaction traits in hosts and
44 parasites – resistance and infectivity, respectively (1,2). Coevolution is fundamental for
45 understanding host-parasite interactions and disease dynamics in nature, as the presence of
46 parasites depends on the availability of susceptible hosts. Indeed, host-parasite interactions
47 provide some of the most compelling evidence for the theory of coevolution, often
48 demonstrated through local adaptation experiments (3–6). However, much of this work has
49 focused on the one-host-one-parasite framework, although in nature hosts are rarely infected
50 by a single parasite and often support complex parasite communities (7–10). Despite the
51 growing interest in within-host parasite communities in natural environments, there remains a
52 gap in our understanding of how coevolution can shape these complex communities (11,12).

53 Genetic variation and genotype-genotype specificity in the interaction are prerequisites
54 for coevolution. Indeed, the ability to infect or resist infection can be genotype-dependent:
55 some parasite genotypes can infect only certain host genotypes, while some host genotypes
56 exhibit resistance to specific parasite genotypes (13–15). This variation is maintained by
57 evolutionary mechanisms, such as parasite-imposed negative frequency-dependent selection
58 and arms-race dynamics, which can favour different host genotypes in different populations,
59 contributing to local adaptation (3,15,16). Notably, the outcome of host genotype \times parasite
60 genotype interactions may be altered under multiple parasite attack (17,18), with co-occurring
61 parasites influencing community assembly either directly through parasite-parasite interactions
62 (19,20) or indirectly through host-mediated responses (14,21). If host colonization ability – a
63 trait expected to be shaped by coevolution – is sensitive to co-occurring parasites, then we may
64 expect community assembly to be shaped by both ecological and evolutionary dynamics (22).
65 The community monopolization hypothesis – evoked to explain evolutionary priority effects
66 – predicts that locally adapted resident species can have a competitive advantage over later

67 arriving individuals, potentially influencing parasite community dynamics (23,24). It has been
68 demonstrated that adaptation can reduce competitive dominance with direct consequences for
69 community assembly (24), and that locally adapted parasites can influence the composition of
70 the entire community (25,26).

71 Viruses, similar to other parasites, can form highly diverse communities (20,27–32).
72 As obligate parasites, viral reproduction relies on the virus' ability to infect and hijack host cell
73 machinery (33), making host-virus interactions a key factor in shaping viral communities
74 (14,34,35). Here, to investigate how viral community assembly is influenced by coevolution,
75 we conducted a reciprocal transplant experiment, by placing naïve *Plantago lanceolata*
76 individuals as sentinels in sympatric and allopatric populations during naturally occurring viral
77 epidemics. We sampled the plant individuals at the end of the growth season for small-RNA
78 sequencing to characterize viral communities and used joint species distribution modelling (36)
79 to tease apart the effects of local adaptation, population and host characteristics on viral
80 community assembly. Specifically, we ask: i) Can we detect viral local adaptation? ii) What is
81 the importance of local adaptation in determining viral community assembly? iii) What is the
82 role of population and host characteristics in viral community assembly?

83

84 Materials and Methods

85 Study species

86 The host, *Plantago lanceolata*, is a perennial herb reproducing clonally with side rosettes or
87 sexually with wind-dispersed pollen (37). *Plantago lanceolata* occurs worldwide, and in
88 Finland, *P. lanceolata* can be found mainly in SW Finland. In the Åland Islands (an area
89 spanning 50 × 70 km), *P. lanceolata* forms a large network consisting of over 4000 small
90 fragmented populations (38).

91 The *P. lanceolata* host populations in the Åland Islands harbour complex viral
92 communities (19,20). Five novel *P. lanceolata* infecting viruses have been characterised from
93 this system, and PCR primers have been developed for their detection (14,39,40). Viral
94 symptoms in wild hosts are challenging to identify but can include yellowing or redness of the
95 leaf, curliness and necrotic lesions (40–42). *Plantago lanceolata latent virus* (PILV) infection
96 has been linked to yellowing of the leaf (40,43).

97

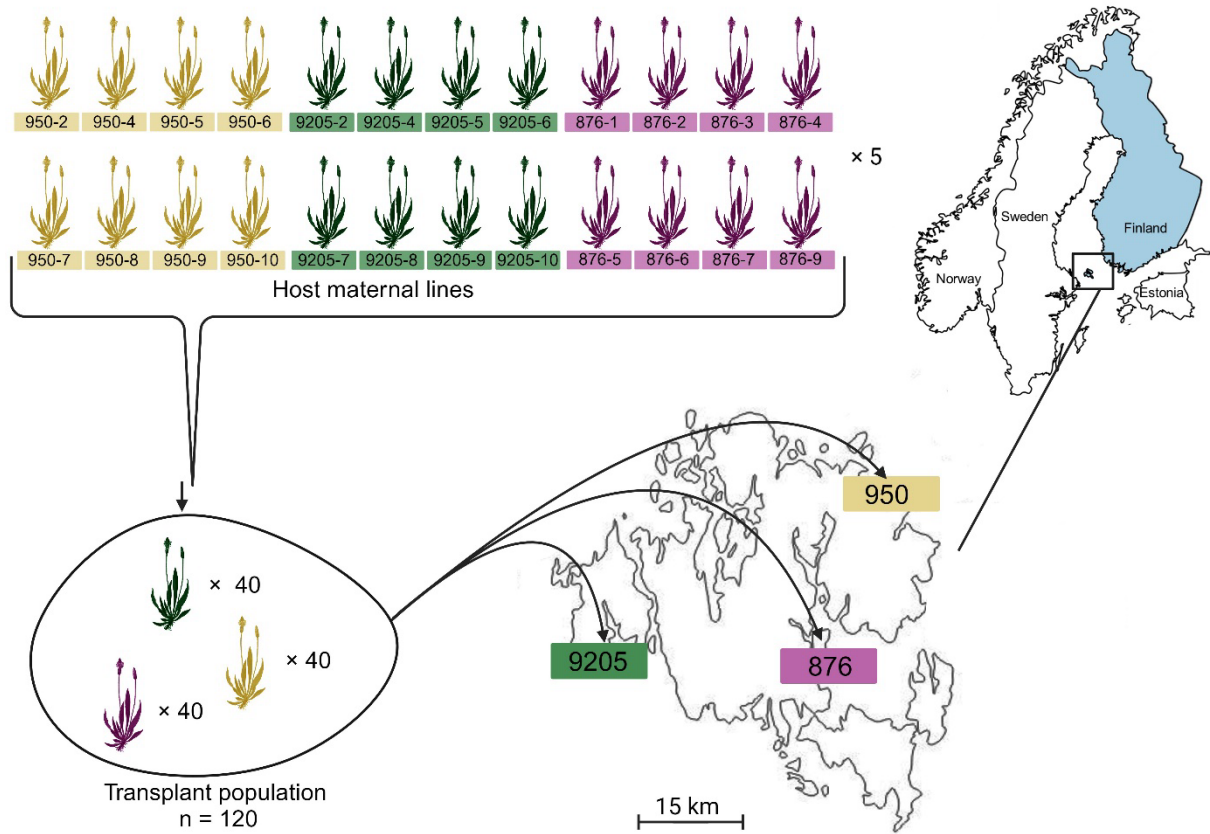
98 Preparation of host plant material and field experiment

99 To investigate the role of local adaptation in viral community assembly, we conducted a
100 reciprocal transplant experiment in three *P. lanceolata* populations (ID: s: 9205, 876, and 950)
101 in the Åland Islands. In autumn 2020, seeds were collected from eight individuals per studied
102 population and germinated in early April 2021 with the aim of obtaining up to 15 offspring per
103 maternal line. The seeds from 24 maternal lines (Supplementary table 1), were sown in peat
104 pots with a 3:1 mixture of potting soil and sand and then placed in a growth chamber with a
105 16:8 h light-dark cycle. After three weeks, the seedlings were transferred to the greenhouse and
106 replanted into 10 cm ×10 cm pots filled with a 1:1 mixture of potting soil and sand. The plants
107 were watered as needed and, when large enough, fertilized weekly with NPK fertilizer (7:2:2).
108 During the growth period in the greenhouse, leaf samples were collected for PCR screening to
109 confirm that each maternal line was virus-free of PILV, *Plantago latent caulimovirus*, *Plantago*
110 *betapartitivirus*, *Plantago enamovirus*, and *Plantago closterovirus*, all of which are among the
111 most common viruses in the Åland Islands populations (39,40). Two weeks prior to the
112 transplant experiment, the plants were treated with fungicide (Bordeaux mixture).

113 In early June 2021, the greenhouse-grown naïve plants were taken to the Åland Islands
114 and placed in their transplant populations. For each maternal line, five offspring were placed

115 in their sympatric *P. lanceolata* population and five in each of the two allopatric populations
116 (Figure 1). For four maternal lines with fewer offspring, priority was given to sympatric
117 placement, and the remaining individuals were distributed among the two allopatric
118 populations (Supplementary table 1). Finally, the experiment consisted of 348 plants across the
119 three transplant populations (Supplementary table 1). The plants were randomly placed among
120 the natural vegetation and kept in pots placed inside plastic boxes (approximately 13 cm × 11
121 cm) to isolate them from the local soil. To minimize within-population spatial effects, we
122 shuffled the plants among the plastic boxes three times per week for the duration of the
123 experiment. The plants were watered as needed.

124 After six weeks of exposure, a 3 cm² piece of leaf tissue was collected for RNA
125 extraction and snap-frozen in liquid nitrogen. At this time, we also recorded host characteristics
126 that prior work suggests could affect viral infections on *P. lanceolata*. Plant size was measured
127 as $n \times A$, where n is the number of leaves and $A = \pi ab$, where a is the half axis of the width of
128 the largest leaf, and b is the half axis of the length of the largest leaf (14,19).



129

130 Figure 1. Reciprocal transplant experiment where *Plantago lanceolata* individuals from 24
 131 maternal lines originating from three populations were transplanted into their sympatric and
 132 two allopatric populations during natural viral epidemics. We placed 40 individuals into
 133 sympatric population and ~80 individuals into two allopatric populations, with a total of 348
 134 plant individuals across three populations in the Åland Islands SW Finland.

135

136 RNA extraction and RNA purification

137 Total RNA was extracted using a modified acid phenol-chloroform extraction protocol (44). A
 138 3 cm² leaf tissue sample was ground in liquid nitrogen, after which 800 µl of warm extraction
 139 buffer was added and mixed thoroughly. The extraction buffer consisted of 2%
 140 hexadecyltrimethylammonium bromide (Sigma-Aldrich USA), 2% of polyvinylpyrrolidone K-
 141 30 (MW 40 000, Sigma-Aldrich USA), 100 mM of Tris-HCl (pH 8.0, Thermo Fisher Scientific,
 142 USA), 25 mM of Ethylenediaminetetraacetic acid (pH 8.9, Sigma-Aldrich, USA), 2.0 M of
 143 NaCl (Sigma-Aldrich, USA) and 2% of β-mercaptoethanol (Sigma-Aldrich, USA). Next, 800
 144 µl of acid phenol-chloroform-isoamyl alcohol (IAA; 25:24:1) was added, and the sample was

145 centrifuged at 13500 rpm for 15 minutes at RT. The supernatant was transferred to a clean tube,
146 mixed with 1 ml phenol-chloroform-IAA and centrifuged under the same conditions. RNA was
147 precipitated by adding 160 μ l of 10 M LiCl and incubating overnight at +4 °C. The following
148 day, samples were purified with chloroform-IAA (24:1) purification step and washed twice
149 with ethanol. The RNA pellet was resuspended in 25 μ l of nuclease-free water and treated with
150 Ambion® DNA-*free*™ DNA removal Kit (Invitrogen, USA). RNA concentration was
151 measured using Nanodrop 2000 (Thermo Fischer Scientific, USA) and Qubit (Thermo Fischer
152 Scientific, USA), and RNA was stored at -80 °C.

153

154 Small-RNA sequencing and bioinformatic pipeline

155 To identify the viral communities present in the sentinel plants, we assigned the samples to
156 small-RNA (sRNA) sequencing. From the 348 sampled experimental plants, we randomly
157 selected samples from three individuals from each maternal line from each transplant
158 population to be assigned for sRNA sequencing. From maternal line 876-4, we sequenced three
159 samples from the sympatric transplant population but only one sample from one of the
160 allopatric populations, resulting in 211 samples assigned for sRNA sequencing. The RNA
161 extracted from the selected samples was diluted with nuclease-free water and sent to the
162 sequencing facility according to the sequencing company's instructions (Fasteris SA,
163 Switzerland).

164 The sRNA sequencing and library preparation were carried out at Fasteris SA
165 (Switzerland). Small-RNA cDNA libraries were prepared using QIAseq miRNA Library Kit
166 (Qiagen) according to Fasteris SA Small RNA-Seq Gel-free protocol with 100 ng of total RNA.
167 Sequencing was performed using Illumina NovaSeq 6000 (Illumina Inc, San Diego, California,
168 USA) and targeted insert sizes from 0 nt to 43 nt with an average library yield of 1779 Mb.

169 Inserts with sizes from 20 nt to 25 nt were selected for bioinformatic analyses. Sequencing
170 adapter removal was done using Trimmomatics software (45), and the reads were de novo
171 assembled to contigs using VirusDetect software (46). VirusDetect software conducts
172 BLASTX and BLASTN searches against curated plant virus database (vrl_Plants_248_U100)
173 of VirusDetect for each sample separately. We used default parameters BLASTX and
174 BLASTN searches, default similarity 25 % and p-value 1e-5. We then assigned the obtained
175 contigs to virus family level for the statistical analyses (Supplementary table 2).

176

177 Statistical analysis

178 All statistical analyses were conducted in R (version 4.2.2; (47). To test whether local
179 adaptation influenced host infection status (infected by any studied virus= 1, not infected by
180 any studied virus = 0), we fitted generalized linear mixed models (GLMM) using the
181 "glmmTMB" R-package (48) with binomial distribution and logit link function. Specifically,
182 we constructed GLMMs to test the two key metrics of local adaptation: i) local *vs.* foreign and
183 ii) home *vs.* away (49,50). For the local *vs.* foreign model (LF), a categorical variable
184 representing sympatry or allopatry, nested within transplant population, was included as a fixed
185 effect. Seed origin population and plant size were included as additional fixed effects and
186 maternal line nested within seed origin population was included as a random effect to account
187 for genetic variation among hosts. For the home *vs.* away model (HA), the model structure was
188 identical, except that the categorical variable of sympatry or allopatry was nested within seed
189 origin population and included as a fixed effect. Model assumptions were assessed using R-
190 package "DHARMA" (51). The significance of the main effects were evaluated using Wald χ^2
191 tests (function "Anova" in R-package "car"; (52). For significant effects, pairwise comparisons
192 of the estimated marginal means were performed using functions "contrasts" and "emmeans"

193 from the R-package “emmeans” (version 1.8.8; (53), applying Tukey’s method for multiple
194 comparisons.

195 To investigate the effects of local adaptation, population and host characteristics on
196 within-host viral diversity, while also accounting for viral (co-)occurrence patterns in the
197 transplant experiment, we implemented Joint Species Distribution Modelling (JSDM) using
198 the hierarchical modelling of species communities (HMSC) framework (54,55). HMSC is a
199 hierarchical generalized linear mixed model with Bayesian inference and allows the analysis
200 of multiple species’ responses to ecological variables while incorporating species- and
201 community-level parameters and accounting for covariation among species. The response
202 variables in our HMSC model were the occurrences of the three most prevalent virus families:
203 *Caulimoviridae*, *Partitiviridae* and *Pospivirodae*. As fixed effect predictors, we included 1)
204 maternal line ID, 2) seed origin population, 3) sympatry/allopattery, 4) plant size, and 5) signs
205 of herbivory. Transplant population was included as a random effect. Including
206 sympatry/allopattery as a fixed effect allowed us to directly estimate the effect of local adaptation
207 in our model. We used four separate Markov chain Monte Carlo (MCMC) chains to sample the
208 posterior distribution. Each chain was run for 1 875 000 iterations, and the first 625 000 were
209 discarded as burn-in. Subsequently, the remaining iterations were thinned by 5000, resulting in
210 250 posterior samples per chain. Finally, we obtained a total of 1000 posterior samples across
211 all four chains. The model fit was evaluated by examining explanatory and predictive
212 performance via ten-fold cross-validation, using Tjur’s coefficient of determination (Tjur R^2)
213 and area under the curve (AUC), respectively. The HMSC analyses were ran using the R-
214 package “Hmsc” (version 3.0-14).

215

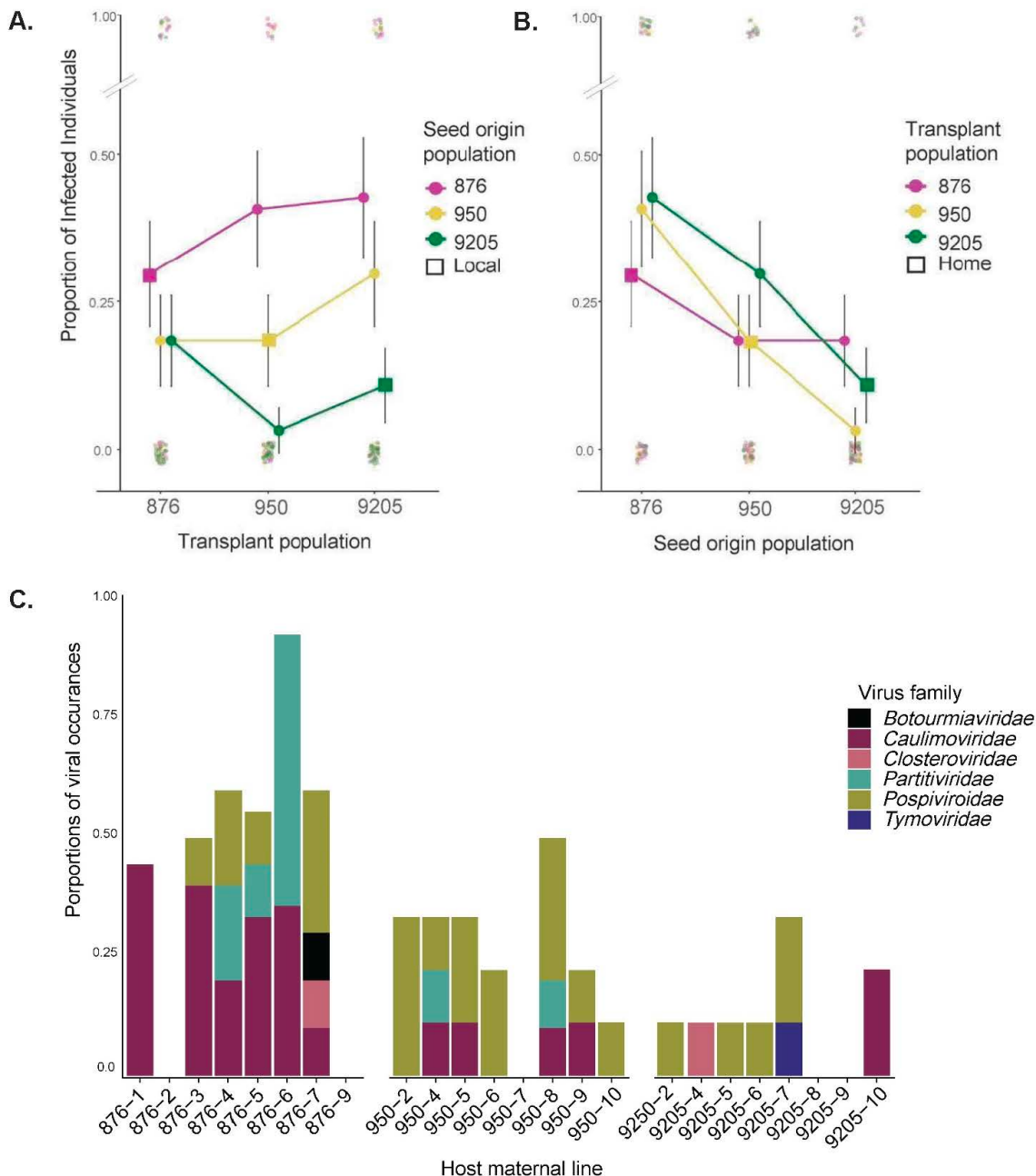
216

217 Results

218 Description of the sRNA sequencing data

219 From the 211 sequenced individuals, the sRNA sequencing yielded on average 23,799,485
220 reads per plant tissue sample (min 17,364,260; max 49,152,805; SD 7,738,962). The
221 VirusDetect pipeline assembled 2374 contigs ranging from 41 to 2080 nt in length (mean length
222 of 159 nt and SD 163 nt). Of these, 11% of contigs had virus-specific BLASTN hits with 80–
223 100% identity (mean 93%), while 89% had BLASTX hits with 22–100% identity (mean 67%).

224 In total, we assembled 1151 plant virus-associated contigs across the 211 individuals,
225 representing six plant virus families: *Tymoviridae*, *Botourmiaviridae*, *Closteroviridae*,
226 *Partitiviridae*, *Caulimoviridae* and *Pospiviroidae* (Figure 2C, Supplementary table 2). From
227 each family, we identified 1 to 3 virus genera and 3 to 842 contigs for each genus. At the species
228 level, we acquired BLAST hits to 1 to 15 species, depending on the virus genus (Supplementary
229 table 2). Overall, 26% of the host individuals were infected, and of those 86% were colonized
230 by one virus family and 14% by two virus families. The most prevalent families were
231 *Caulimoviridae* and *Pospiviroidae* (both in 43% of the infected individuals), whereas
232 *Tymoviridae* and *Botourmiaviridae* were the rarest (both in 2% of the infected individuals;
233 Figure 2C).



234

235 Figure 2. Proportions of virus infected *Plantago lanceolata* host individuals in a reciprocal
236 transplant experiment using (A) local vs. foreign, (B) home vs. away metrics of local
237 adaptation, and (C) infection pattern across host maternal (n = 24) line grouped by seed origin
238 population. In panel A, colours indicate the seed origin populations and the squares mark the
239 local host. In panel B, the colours represent the transplant populations and the squares mark
240 the home habitat of the host (purple = seed origin/transplant population 876, yellow = seed
241 origin/transplant population 950, and green = seed origin/transplant population 9205). In panel
242 C colours represent the six virus families detected with sRNA sequencing.

243

244 Analysis of viral local adaptation: local *vs.* foreign
245 Using the local *vs.* foreign criterion, we observed indications of viral local adaptation in
246 transplant population 876, where local hosts had higher infection rates than foreign hosts. A
247 similar trend was observed in population 950, where local hosts showed the second-highest
248 infection rates (Figure 2A). Conversely, in population 9205, local hosts harboured fewer
249 infections than foreign hosts – suggesting viral maladaptation. However, the GLMM (LF) did
250 not provide statistical support for these trends (Wald $X^2 = 1.53$, $P = 0.673$; Table 1). Seed
251 origin populations differed significantly in infection rates (Wald $X^2 = 7.37$, $P = 0.025$; Table
252 1), with individuals originating from population 9205 having significantly fewer infections
253 than those originating from population 876 (Figure 2A, Supplementary table 3A; estimate =
254 2.071, SE = 0.778, z-ratio = 2.661, $P = 0.021$).

255 Table 1. Type II Wald X^2 test for Generalized linear mixed model estimating the effects of plant
256 size, seed origin population, transplant population and local *vs.* foreign metric of local
257 adaptation on host infection status (1=infected, 0=uninfected) in a reciprocal transplant
258 experiment in the Åland Islands (model LF).

259

Fixed effect	Wald X^2	Df	p-value
Plant size	1.71	1	0.190
Seed origin population	7.37	2	0.025
Transplant population	1.99	2	0.369
Transplant population: sympatry/allopatry	1.53	3	0.673

260

261 Analysis of viral local adaptation: home *vs.* away
262 Applying the home *vs.* away criterion, we found no evidence of viral local adaptation (Figure
263 2B). Hosts from populations 876 and 950 had lower infection rates in their respective home
264 populations than in their away populations, suggesting viral maladaptation (Figure 2B). Our
265 statistical analysis (model HA) did not detect significant differences in infection rates between

266 home and away habitats. However, model coefficients for the “sympatry“ term nested within
267 seed origin population were lower, suggesting higher infection rates in away habitats
268 (Supplementary table 4). Additionally, seed origin population significantly influenced host
269 infection status (Wald $X^2 = 9.09$, $P=0.010$; Table 2). Post hoc comparisons showed that
270 individuals from population 876 had significantly higher infection rates than those from
271 population 9205 (estimate = 1.818, SE = 0.649, z-ratio = 2.802, $P = 0.014$; Supplementary table
272 3B., Figure 2B and C).

273 Table 2. Type II Wald X^2 test for Generalized linear mixed model testing for the effects of plant
274 size, seed origin population, transplant population and home vs. away metric of local adaptation
275 on host infection status (1=infected, 0=uninfected) in a reciprocal transplant experiment in the
276 Åland Islands (model HA).

277

Fixed effect	Wald X^2	Df	p-value
Plant size	1.71	1	0.190
Seed origin population	9.09	2	0.010
Transplant population	1.64	2	0.438
Seed origin population: sympatry/allopatry	1.53	3	0.673

278

279 Analysis of viral (co-)occurrence patterns

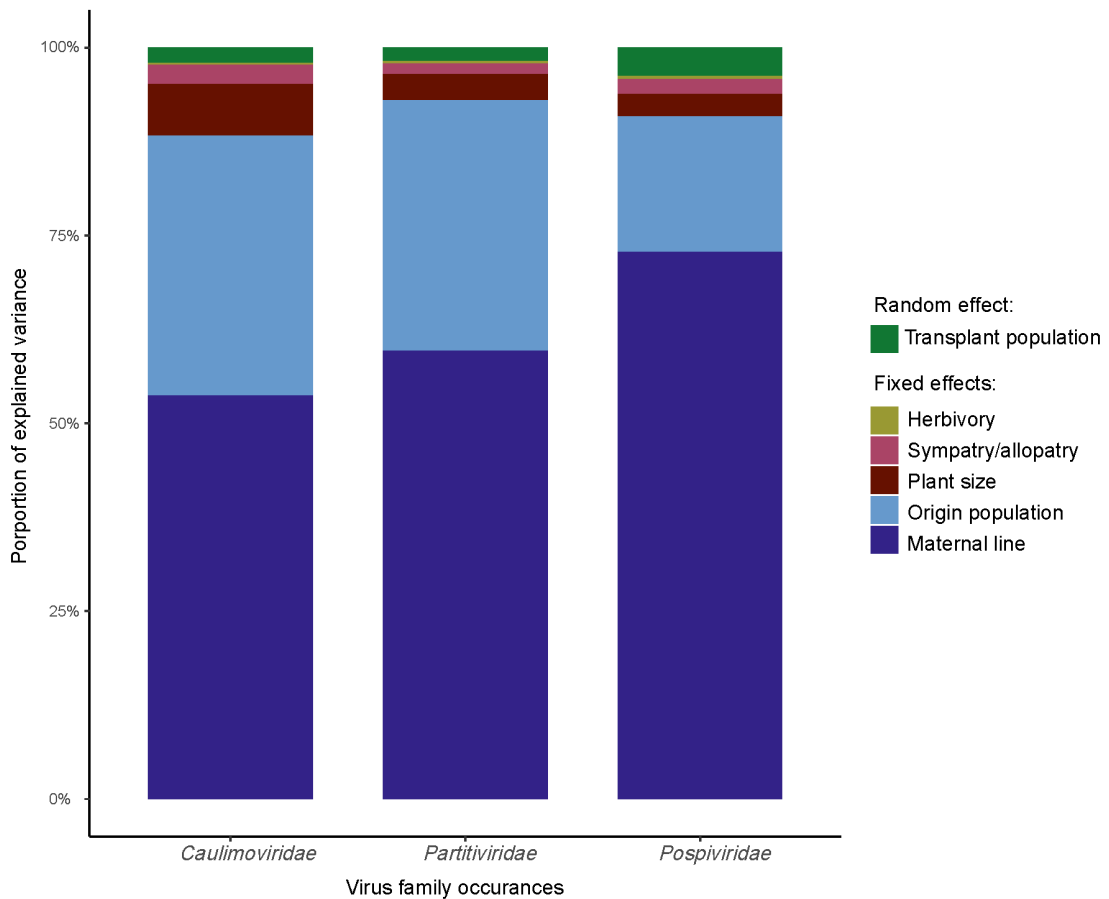
280 We applied the HMSC approach to investigate the factors influencing the (co-)occurrence of
281 the detected virus families in a local adaptation experiment. The model predicted virus family
282 occurrences well, although model performance varied among virus families (Supplementary
283 table 5). Tjur R^2 and AUC were used to quantify the explanatory and predictive performance
284 of the model, with a mean Tjur R^2 of 0.27 (range among the detected virus families 0.10-0.47)
285 and a mean AUC of 0.89 (0.80-0.98). The predictive power of the model was based on ten-fold
286 cross-validations, where the mean Tjur R^2 was 0.19 (range 0.01 - 0.4) and the mean AUC was
287 0.74 (range 0.54-0.88; Supplementary table 5) varying among virus families.

288 In terms of contributions to the explained variation in our HMSC model, host maternal
289 line was the strongest determinant of viral occurrences, explaining on average 62% of the
290 variance. However, the effect varied among virus families and was most pronounced for
291 *Pospiviroidae* (73%) and less important in explaining *Partitiviridae* (60%) and *Caulimoviridae*
292 (54%) occurrences (Figure 3, Supplementary table 6). For example, maternal line 876-6,
293 displayed the highest infection rates, with 89% of the individuals infected (Figure 2C). Seed
294 origin population was the second most important predictor, explaining on average of 29% of
295 the variance. The effect of host maternal line varied among virus families, with a more
296 pronounced role for *Caulimoviridae* (35%) and *Partitiviridae* (33%), while being less
297 important for explaining the occurrences of *Pospiviroidae* (18%; Figure 3, Supplementary table
298 6). Consistent with this, individuals from seed origin population 876 harboured 50% of all
299 detected viral infections, whereas individuals originating from population 9205 harboured only
300 16% of all infections (Figure 2C).

301 Host plant size accounted for an average of 4% of the variation in viral occurrences,
302 with the strongest effect observed for *Caulimoviridae* (7%). Local adaptation
303 (sympatry/allopatry) had a smaller role in contributing to explained variation, accounting for
304 2% on average across virus families (Figure 3, Supplementary table 6). Herbivory had minimal
305 effect, explaining only 0% to 0.1% of the viral occurrences. The random effect of transplant
306 population explained on average 2% of the variation across virus families and was slightly
307 more important in explaining *Pospiviroidae* occurrences (4%, Figure 3, Supplementary table
308 6). Residual correlations among virus families at the random level were not significant,
309 suggesting that after accounting for the effects of the fixed explanatory variables, viral
310 occurrences were not influenced by interactions between virus families.

311

312 Figure 3. Variance partitioning of the fixed and random effects in the Hierarchical Modelling
313 of Species Communities model for the three most prevalent virus families (*Caulimoviridae*,
314 *Partitiviridae*, *Pospiviridae*) in the reciprocal transplant experiment. The six variables
315 explaining the occurrences the three virus families were: maternal line, seed origin population,
316 plant size, sympathy/allopsty, herbivory and transplant population (random effect).



317
318

319 Discussion

320 Here, we used a reciprocal transplant experiment combined with sRNA sequencing and JSDM
321 modelling to investigate the role of local adaptation in shaping within-host viral (co-
322)occurrences. Although we observed trends suggesting viral local adaptation and maladaptation
323 when applying the local *vs.* foreign and home *vs.* away criteria, the effects were not statistically
324 significant. Instead, we found host maternal line and host seed origin population to be the most
325 important determinants of host infection status and viral community structure. The strength of

326 these effects varied across virus families, indicating virus-specific assembly processes and
327 variation in the extent to which coevolution shapes these interactions. Jointly our results
328 identify key drivers of viral community assembly and provide insight into how within-host
329 dynamics could scale up to predict the ecological and evolutionary consequences of disease in
330 natural systems.

331 Using sRNA sequencing, we detected viruses from six virus families, five of which
332 have been previously identified from this system (20,43). Overall, 21% of the sampled sentinel
333 plants were infected, exhibiting a lower infection rate than previously reported from hosts in
334 this system (20,43). Despite the low overall infection prevalence, we found individuals
335 originating from population 876 harbouring significantly higher infection rates than those from
336 population 9205. Viral community composition also varied among seed origin populations and
337 among maternal lines. Individuals from seed origin population 876 harboured viruses from five
338 different virus families (*Caulimoviridae*, *Pospiviroidae*, *Partitiviridae*, *Botourmiaviridae* and
339 *Closteroviridae*), whereas individuals from population 950 were infected by only three virus
340 families (*Pospiviroidae*, *Caulimoviridae* and *Partitiviridae*). The overall lower infection
341 prevalence may be due to differences in exposure time to viral epidemics and additionally, viral
342 prevalence may vary annually due to several factors, such as temperature, humidity and vector
343 behaviour — components of natural systems that are difficult to control in a field experiment
344 (56–58).

345 Using a reciprocal transplant experimental approach, we were able to apply the two key
346 metrics of local adaptation: local *vs.* foreign and home *vs.* away. While we observed signs of
347 viral local adaptation in transplant population 876 under the local *vs.* away criterion, the pattern
348 was not statistically significant (GLMM LF). Similarly, analysis on the home *vs.* away metric
349 showed no statistically significant effect of local adaptation on host infection status (GLMM
350 HA). In line with these results, when investigating the effects of local adaptation on viral (co-

351)occurrence patterns with JSDM in the HMSC framework, we found local adaptation to explain
352 on average only 2.3% of the viral occurrences. However, when using the home *vs.* away
353 criterion (GLMM HA), individuals from seed origin populations 876 and 950 harboured the
354 lowest infection rates in their home populations, suggesting viral maladaptation. Patterns of
355 maladaptation are not unexpected given the dynamic, cyclic nature of coevolutionary
356 interactions between the host and its parasite (59). In the Aland Islands *P. lanceolata*
357 populations are highly fragmented, and the connectivity levels of the populations vary (60,61)
358 and consequently too high or low gene flow between populations could facilitate parasite
359 maladaptation (59,62–64). Previous studies have shown that well-connected host populations
360 are less affected by disease (65,66), a phenomenon that is likely due to higher resistance
361 diversity in these populations maintained by gene flow (61).

362 Seed origin population was a strong predictor of host infection status. Individuals
363 originating from population 876 were more frequently infected and harboured the most diverse
364 viral communities. In contrast, hosts from population 9205 exhibited high resistance to viral
365 infection and consequently harboured less complex viral communities. Our HMSC analysis
366 mirrored these findings, identifying maternal line and seed origin population as the strongest
367 determinants of viral occurrence across virus families, explaining on average 62% and 29% of
368 the variation, respectively (Figure 3). The variation in infection rates among host origin
369 populations, together with the strong maternal line effects for viral occurrences across virus
370 families, highlights host genetic diversity as a key driver of viral community assembly and
371 composition in this system. Although evidence for viral local adaptation was limited, the
372 variation in infections prevalence among host maternal lines indicates strong potential for
373 coevolution, as genetic variation is a main driver of coevolution (67–69). Moreover, high host
374 genetic diversity in natural populations can mitigate disease risk, a phenomenon known as the
375 monoculture effect (70,71).

376 Hosts encounter a myriad of parasites throughout their lives (43,72–74), and these
377 interactions can have far-reaching consequences for host-parasite coevolution and population
378 dynamics (75). Despite this, much of the research on local adaptation has focused on pairwise
379 host-parasite interactions (76–78), with little focus on the role of parasite communities in
380 coevolutionary processes. To our knowledge, our study is among the first to study viral local
381 adaptation within a community ecology framework. After accounting for host attributes, we
382 found no evidence of virus-virus interactions shaping within-host viral diversity. Instead, host
383 characteristics, represented by maternal line and host seed origin population, emerged as the
384 most important predictor of viral community structure and host infection status. Our findings
385 highlight the importance of host genetic variation in shaping viral communities and contribute
386 to the growing field of viral community ecology research. Understanding the drivers of
387 complex host-parasite interactions and processes at the community level is essential for
388 predicting how disease dynamics scale up from individuals to populations and understanding
389 the ecological and evolutionary conditions from which novel viral diseases may emerge.

390

391 Acknowledgements

392 We thank Krista Raveala, Aura Palonen, Suvi Sallinen, Marijke Iso-Kokkila and Jere Lentonen
393 for the help with the transplant experiment and RNA extractions. We thank Suvi Sallinen for
394 the help with statistical analysis. The CSC – IT Center for Science, Finland, is acknowledged
395 for computational resources. The work was funded by grants from the European Research
396 Council (AdG 101097545 Co-EvoChange), and Academy of Finland (334276, 362242) to A.-
397 L.L. and Academy of Finland (321441) to H.S.

398

399 Author contributions

400 M.J., H.S. and A.-L.L. designed the study. M.J. performed the field experiment, data collection,
401 and statistical analysis. M.J., H.S. and A-L.L. prepared the manuscript.

402 Conflict of Interest

403 The authors declare no conflict of interests.

404 Data availability Statement

405 The data and R scripts used in this study have been submitted to GitHub
406 (<https://github.com/mailijahoki/ViRAL21>).

407

408 References

- 409 1. Buckingham LJ, Ashby B. Coevolutionary theory of hosts and parasites. *J Evol Biol.* 410 2022;35(2):205–24.
- 411 2. Thompson JN, Cunningham BM. Geographic structure and dynamics of coevolutionary 412 selection. *Nature.* 2002;417(6890):735–8.
- 413 3. Decaestecker E, Gaba S, Raeymaekers JAM, Stoks R, Kerckhoven LV, Ebert D, et al. 414 Host-parasite ‘Red Queen’ dynamics archived in pond sediment. *Nature.* 415 2007;450(7171):870–3.
- 416 4. Greischar MA, Koskella B. A synthesis of experimental work on parasite local adaptation. 417 *Ecol Lett.* 2007;10(5):418–34.
- 418 5. Kaltz O, Shykoff JA. Local adaptation in host–parasite systems. *Hered* 1998 814. 1998 Oct 419 1;81(4):361–70.
- 420 6. Dybdahl MF, Storfer A. Parasite local adaptation: Red Queen versus Suicide King. *Trends* 421 *Ecol Evol.* 2003 Oct 1;18(10):523–30.
- 422 7. Johnson PTJ, Hoverman JT. Parasite diversity and coinfection determine pathogen 423 infection success and host fitness. *Proc Natl Acad Sci U S A.* 2012 June 5;109(23):9006– 424 11.

425 8. Ben-Ami F, Mouton L, Ebert D. The effects of multiple infections on the expression and
426 evolution of virulence in a *Daphnia*-endoparasite system. *Evolution*. 2008;62(7):1700–11.

427 9. Tollenaere C, Susi H, Nokso-Koivisto J, Koskinen P, Tack A, Auvinen P, et al. SNP Design
428 from 454 Sequencing of *Podosphaera plantaginis* Transcriptome Reveals a Genetically
429 Diverse Pathogen Metapopulation with High Levels of Mixed-Genotype Infection. *PLoS
430 ONE*. 2012 Dec 27;7(12).

431 10. Griffiths EC, Pedersen AB, Fenton A, Petchey OL. The nature and consequences of
432 coinfection in humans. *J Infect*. 2011 Sept;63(3):200–6.

433 11. Betts A, Gray C, Zelek M, MacLean RC, King KC. High parasite diversity accelerates host
434 adaptation and diversification. *Science*. 2018;360(6391):907–11.

435 12. Hall AR, Ashby B, Bascompte J, King KC. Measuring Coevolutionary Dynamics in
436 Species-Rich Communities. *Trends Ecol Evol*. 2020 June 1;35(6):539–50.

437 13. Hily JM, Poulicard N, Mora MÁ, Pagán I, García-Arenal F. Environment and host
438 genotype determine the outcome of a plant–virus interaction: from antagonism to
439 mutualism. *New Phytol*. 2016 Jan 1;209(2):812–22.

440 14. Sallinen S, Norberg A, Susi H, Laine AL. Intraspecific host variation plays a key role in
441 virus community assembly. *Nat Commun*. 2020;11(1):1–11.

442 15. Gandon S. Local adaptation and the geometry of host-parasite coevolution. *Ecol Lett*.
443 2002;5(2):246–56.

444 16. Woolhouse MEJ, Webster JP, Domingo E, Charlesworth B, Levin BR. Biological and
445 biomedical implications of the co-evolution of pathogens and their hosts. *Nat Genet*.
446 2002;32(4):569–77.

447 17. Tollenaere C, Susi H, Laine AL. Evolutionary and Epidemiological Implications of
448 Multiple Infection in Plants. *Trends Plant Sci*. 2016 Jan 1;21(1):80–90.

449 18. Karvonen A, Fenton A, Sundberg LR. Sequential infection can decrease virulence in a
450 fish–bacterium–fluke interaction: Implications for aquaculture disease management. *Evol
451 Appl*. 2019 Dec 1;12(10):1900–11.

452 19. Jokinen M, Sallinen S, Jones MM, Sirén J, Guilbault E, Susi H, et al. The first arriving
453 virus shapes within-host viral diversity during natural epidemics. *Proc R Soc B [Internet]*.
454 2023 Sept 13 [cited 2023 Nov 30];290(2006). Available from:
455 <https://royalsocietypublishing.org/doi/10.1098/rspb.2023.1486>

456 20. Norberg A, Susi H, Sallinen S, Baran P, Clark NJ, Laine AL. Direct and indirect viral
457 associations predict coexistence in wild plant virus communities. *Curr Biol*. 2023 May
458 8;33(9):1665–1676.e4.

459 21. Tollenaere C, Susi H, Laine AL. Evolutionary and Epidemiological Implications of
460 Multiple Infection in Plants. *Trends Plant Sci*. 2016 Jan 1;21(1):80–90.

461 22. Gorter FA, Manhart M, Ackermann M. Understanding the evolution of interspecies
462 interactions in microbial communities. *Philos Trans R Soc B [Internet]*. 2020 May 11 [cited

463 2024 Oct 14];375(1798). Available from:
464 <https://royalsocietypublishing.org/doi/10.1098/rstb.2019.0256>

465 23. Urban MC, De Meester L. Community monopolization: local adaptation enhances priority
466 effects in an evolving metacommunity. *Proc R Soc B Biol Sci.* 2009 Dec
467 7;276(1676):4129–38.

468 24. Nadeau CP, Farkas TE, Makkay AM, Papke RT, Urban MC. Adaptation reduces
469 competitive dominance and alters community assembly. *Proc R Soc B [Internet].* 2021 Feb
470 24 [cited 2023 Apr 14];288(1945). Available from:
471 <https://royalsocietypublishing.org/doi/10.1098/rspb.2020.3133>

472 25. Pantel JH, Duvivier C, Meester LD. Rapid local adaptation mediates zooplankton
473 community assembly in experimental mesocosms. *Ecol Lett.* 2015;18(10):992–1000.

474 26. Gómez P, Paterson S, De Meester L, Liu X, Lenzi L, Sharma MD, et al. Local adaptation
475 of a bacterium is as important as its presence in structuring a natural microbial community.
476 *Nat Commun [Internet].* 2016 [cited 2024 Oct 11]; Available from:
477 www.nature.com/naturecommunications

478 27. Breitbart M, Hewson I, Felts B, Mahaffy JM, Nulton J, Salamon P, et al. Metagenomic
479 analyses of an uncultured viral community from human feces. *J Bacteriol.* 2003
480 Oct;185(20):6220–3.

481 28. Brum JR, Ignacio-espinoza JC, Roux S, Doulcier G, Acinas SG, Alberti A, et al. Ocean
482 Viral Communities. *Science.* 2015;348(6237):1261411–98.

483 29. Durham DM, Sieradzki ET, Ter Horst AM, Santos-Medellín C, Winston C, Bess A, et al. Substantial differences in soil viral community composition within and among four
484 Northern California habitats. *ISME Commun* 2022 21. 2022 Oct 13;2(1):1–5.

485 30. Pratama AA, van Elsas JD. The ‘Neglected’ Soil Virome – Potential Role and Impact. *Trends Microbiol.* 2018;26(8):649–62.

486 31. Rwahnih MA, Daubert S, Úrbez-Torres JR, Cordero F, Rowhani A. Deep sequencing
487 evidence from single grapevine plants reveals a virome dominated by mycoviruses. *Arch Virol.* 2011;156(3):397–403.

488 32. Yang K, Wang X, Hou R, Lu C, Fan Z, Li J, et al. Rhizosphere phage communities drive
489 soil suppressiveness to bacterial wilt disease. *Microbiome.* 2023;11(1):1–18.

490 33. Christiaansen A, Varga SM, Spencer JV. Viral manipulation of the host immune response. *Curr Opin Immunol.* 2015;36:54.

491 34. Coloma S, Gaedke U, Sivonen K, Hiltunen T. Frequency of virus-resistant hosts determines
492 experimental community dynamics. *Ecology.* 2019;100(1):1–10.

493 35. Roossinck MJ, Bazán ER. Symbiosis: Viruses as Intimate Partners. *Annu Rev Virol.* 2017
494 Sept 29;4:123–39.

499 36. Norberg A, Abrego N, Blanchet FG, Adler FR, Anderson BJ, Anttila J, et al. A
500 comprehensive evaluation of predictive performance of 33 species distribution models at
501 species and community levels. *Ecol Monogr.* 2019 Aug 1;89(3):e01370.

502 37. Sagar GR, Harper JL. *Plantago Major L.*, *P. Media L.* and *P. Lanceolata L.* *J Ecol.* 1964
503 Mar;52(1):189.

504 38. Ojanen SP, Nieminen M, Meyke E, Pöyry J, Hanski I. Long-term metapopulation study of
505 the Glanville fritillary butterfly (*Melitaea cinxia*): Survey methods, data management, and
506 long-term population trends. *Ecol Evol.* 2013 Oct 1;3(11):3713–37.

507 39. Susi H, Laine AL, Filloux D, Krabberger S, Farkas K, Bernardo P, et al. Genome sequences
508 of a capulavirus infecting *Plantago lanceolata* in the Åland archipelago of Finland. *Arch
509 Virol.* 2017 July 1;162(7):2041–5.

510 40. Susi H, Filloux D, Frilander MJ, Roumagnac P, Laine A liisa. Diverse and variable virus
511 communities in wild plant populations revealed by metagenomic tools. 2019;

512 41. Adams IP, Skelton A, Macarthur R, Hodges T, Hinds H, Flint L, et al. Carrot yellow leaf
513 virus is associated with carrot internal necrosis. *PLoS ONE.* 2014 Nov 3;9(11).

514 42. Biswas KK, Bhattacharyya UK, Palchoudhury S, Balram N, Kumar A, Arora R, et al.
515 Dominance of recombinant cotton leaf curl Multan-Rajasthan virus associated with cotton
516 leaf curl disease outbreak in northwest India. *PLOS ONE.* 2020 Apr 1;15(4):e0231886.

517 43. Susi H, Filloux D, Frilander MJ, Roumagnac P, Laine AL. Diverse and variable virus
518 communities in wild plant populations revealed by metagenomic tools. *PeerJ* [Internet].
519 2019 [cited 2020 Feb 19];2019(1). Available from: <http://doi.org/10.7717/peerj.6140>

520 44. Chang S, Puryear J, Cairney J. A simple and efficient method for isolating RNA from pine
521 trees. *Plant Mol Biol Report.* 1993;11(2):113–6.

522 45. Bolger AM, Lohse M, Usadel B. Genome analysis Trimmomatic: a flexible trimmer for
523 Illumina sequence data. 2014;30(15):2114–20.

524 46. Zheng Y, Gao S, Padmanabhan C, Li R, Galvez M, Gutierrez D, et al. VirusDetect: An
525 automated pipeline for efficient virus discovery using deep sequencing of small RNAs.
526 *Virology.* 2017 Jan 1;500:130–8.

527 47. R Foundation for Statistical Computing, Vienna A. R: A language and environment for
528 statistical computing. 2022; Available from: <https://www.r-project.org/>

529 48. Brooks ME, Kristensen K, Van Benthem KJ, Magnusson A, Berg CW, Nielsen A, et al.
530 glmmTMB Balances Speed and Flexibility Among Packages for Zero-inflated Generalized
531 Linear Mixed Modeling. *R J.* 2017;9:2.

532 49. Kawecki TJ, Ebert D. Conceptual issues in local adaptation. *Ecol Lett.* 2004 Dec
533 1;7(12):1225–41.

534 50. Blanquart F, Kaltz O, Nuismer SL, Gandon S. A practical guide to measuring local
535 adaptation. *Ecol Lett.* 2013 Sept;16(9):1195–205.

536 51. Hartig F. DHARMA: Residual Diagnostics for Hierarchical (Multi-Level / Mixed)
537 Regression Models. 2022; Available from: <https://cran.r-project.org/package=DHARMA>

538 52. Fox J, Weisberg S. An R Companion to Applied Regression. Sage Publ. 2019;

539 53. Russell V, Lenth RV, BB [ctb], PB [ctb], IGV [ctb], MH [ctb], MJ [ctb], JL [ctb], FM [ctb],
540 JP [ctb], HR [ctb], SH. Package “Emmeans”. 2018;

541 54. Ovaskainen O, Tikhonov G, Norberg A, Guillaume Blanchet F, Duan L, Dunson D, et al.
542 How to make more out of community data? A conceptual framework and its
543 implementation as models and software. *Ecol Lett.* 2017 May 1;20(5):561–76.

544 55. Ovaskainen O, Abrego N. Joint Species Distribution Modelling [Internet]. Cambridge
545 University Press; 2020 [cited 2022 Oct 17]. Available from:
546 <https://www.cambridge.org/core/product/identifier/9781108591720/type/book>

547 56. Trebicki P. Climate change and plant virus epidemiology. *Virus Res.*
548 2020;286(June):198059.

549 57. Kendig AE, Borer ET, Mitchell CE, Power AG, Seabloom EW. Characteristics and drivers
550 of plant virus community spatial patterns in US west coast grasslands. *Oikos.* 2017 Sept
551 1;126(9):1281–90.

552 58. Jeger MJ, Fereres A, Malmstrom CE, Mauck KE, Wintermantel WM. Epidemiology and
553 Management of Plant Viruses Under a Changing Climate. *Phytopathology.* 2023 Nov
554 4;113(9):1620–1.

555 59. Kaltz O, Gandon S, Michalakis Y, Shykoff JA. Local maladaptation in the anther-smut
556 fungus *Microbotryum violaceum* to its host plant *Silene latifolia*: Evidence from a cross-
557 inoculation experiment. *Evolution.* 1999;53(2):395–407.

558 60. Jousimo J, Tack AJM, Ovaskainen O, Mononen T, Susi H, Tollenaere C, et al. Ecological
559 and evolutionary effects of fragmentation on infectious disease dynamics. *Science.*
560 2014;344(6189):1289–93.

561 61. Höckerstedt L, Siren JP, Laine AL. Effect of spatial connectivity on host resistance in a
562 highly fragmented natural pathosystem. *J Evol Biol.* 2018;31(6):844–52.

563 62. Gandon S. Local adaptation and the geometry of host-parasite coevolution. *Ecol Lett.*
564 2002;5(2):246–56.

565 63. Hoeksema JD, Forde SE. A meta-analysis of factors affecting local adaptation between
566 interacting species. *Am Nat.* 2008 Mar;171(3):275–90.

567 64. Oppliger A, Vernet R, Baezà M. Parasite local maladaptation in the Canarian lizard
568 *Gallotia galloti* (Reptilia: Lacertidae) parasitized by haemogregarine blood parasite. *J Evol
569 Biol.* 1999;12(5):951–5.

570 65. Höckerstedt L, Numminen E, Ashby B, Boots M, Norberg A, Laine AL. Spatially
571 structured eco-evolutionary dynamics in a host-pathogen interaction render isolated
572 populations vulnerable to disease. *Nat Commun.* 2022;13(1):1–11.

573 66. Carlsson-Granér U, Thrall PH. Host resistance and pathogen infectivity in host populations
574 with varying connectivity. *Evolution*. 2015 Apr 1;69(4):926–38.

575 67. Paterson S, Vogwill T, Buckling A, Benmayor R, Spiers AJ, Thomson NR, et al.
576 Antagonistic coevolution accelerates molecular evolution. *Nature*. 2010 Mar
577 11;464(7286):275–8.

578 68. Buckingham LJ, Ashby B. Coevolutionary theory of hosts and parasites. *J Evol Biol*. 2022
579 Feb 1;35(2):205–24.

580 69. Laine AL, Burdon JJ, Dodds PN, Thrall PH. Spatial variation in disease resistance: From
581 molecules to metapopulations. *J Ecol*. 2011;99(1):96–112.

582 70. Laine AL, Burdon JJ, Dodds PN, Thrall PH. Spatial variation in disease resistance: From
583 molecules to metapopulations. *J Ecol*. 2011 Jan;99(1):96–112.

584 71. Ridenhour BJ, Nuismer SL. Polygenic traits and parasite local adaptation. *Evolution*.
585 2007;61(2):368–76.

586 72. Vayssier-Taussat M, Kazimirova M, Hubalek Z, Hornok S, Farkas R, Cosson JF, et al.
587 Emerging horizons for tick-borne pathogens: From the ‘one pathogen-one disease’ vision
588 to the pathobiome paradigm. *Future Microbiol*. 2015 Dec 1;10(12):2033–43.

589 73. Susi H, Barrès B, Vale PF, Laine AL. Co-infection alters population dynamics of infectious
590 disease. *Nat Commun*. 2015 Jan 8;6(1):1–8.

591 74. Boots M, White A, Best A, Bowers R. The importance of who infects whom: The evolution
592 of diversity in host resistance to infectious disease. *Ecol Lett*. 2012;15(10):1104–11.

593 75. Hall AR, Ashby B, Bascompte J, King KC. Measuring Coevolutionary Dynamics in
594 Species-Rich Communities. *Trends Ecol Evol*. 2020;35(6):539–50.

595 76. Ridenhour BJ, Nuismer SL. Polygenic traits and parasite local adaptation. *Evolution*. 2007
596 Feb;61(2):368–76.

597 77. Laine AL. Detecting local adaptation in a natural plant-pathogen metapopulation: A
598 laboratory vs. field transplant approach. *J Evol Biol*. 2007 Sept;20(5):1665–73.

599 78. Mauck KE, De Moraes CM, Mescher MC. Evidence of Local Adaptation in Plant Virus
600 Effects on Host–Vector Interactions. *Integr Comp Biol*. 2014 July 1;54(2):193–209.

601

602

603

604

605

606

607 **Supplement**

608

609 **Supplementary table 1.** The host maternal lines included in a reciprocal transplant experiment
610 studying viral local adaptation in *Plantago lanceolata* host populations in the Åland Islands
611 during naturally occurring viral epidemics. In the table are included the ID of each maternal
612 line, the ID of the origin population of each maternal line, the ID of the transplant population
613 where the plants were placed during the experiment and the number of individuals, and finally,
614 the number of sequenced individuals.

Maternal line	Seed origin population	Transplant population	No individuals in the experiment	Number of individuals sequenced
876-1	876	876	5	3
876-1	876	950	5	3
876-1	876	9205	5	3
876-2	876	876	5	3
876-2	876	950	5	3
876-2	876	9205	5	3
876-3	876	876	5	3
876-3	876	950	5	3
876-3	876	9205	5	3
876-4	876	876	5	3
876-4	876	950	1	1
876-4	876	9205	0	0
876-5	876	876	5	3
876-5	876	950	4	3
876-5	876	9205	3	3
876-6	876	876	5	3
876-6	876	950	5	3
876-6	876	9205	5	3
876-7	876	876	5	3
876-7	876	950	5	3
876-7	876	9205	5	3
876-9	876	876	5	3
876-9	876	950	5	3
876-9	876	9205	5	3
950-10	950	876	5	3
950-10	950	950	5	3
950-10	950	9205	5	3
950-2	950	876	5	3
950-2	950	950	5	3
950-2	950	9205	5	3
950-4	950	876	5	3
950-4	950	950	5	3
950-4	950	9205	5	3
950-5	950	876	5	3
950-5	950	950	5	3
950-5	950	9205	5	3
950-6	950	876	5	3
950-6	950	950	5	3
950-6	950	9205	5	3
950-7	950	876	5	3
950-7	950	950	5	3
950-7	950	9205	5	3
950-8	950	876	5	3
950-8	950	950	5	3
950-8	950	9205	5	3
950-9	950	876	5	3
950-9	950	950	5	3
950-9	950	9205	5	3

615

616

617

618

619

620

9205-10	9205	876	5	3
9205-10	9205	950	5	3
9205-10	9205	9205	5	3
9205-4	9205	876	5	3
9205-4	9205	950	5	3
9205-4	9205	9205	5	3
9205-5	9205	876	5	3
9205-5	9205	950	5	3
9205-5	9205	9205	5	3
9205-6	9205	876	5	3
9205-6	9205	950	5	3
9205-6	9205	9205	5	3
9205-7	9205	876	5	3
9205-7	9205	950	5	3
9205-7	9205	9205	5	3
9205-8	9205	876	4	3
9205-8	9205	950	5	3
9205-8	9205	9205	5	3
9205-9	9205	876	5	3
9205-9	9205	950	5	3
9205-9	9205	9205	5	3
9250-2	9205	876	5	3
9250-2	9205	950	5	3
9250-2	9205	9205	5	3

621

622

623

624

625

626

627 **Supplementary table 2.** Virus families detected by small-RNA sequencing on *Plantago*
 628 *lanceolata* individuals (n = 211) included in a transplant experiment in the Åland Islands
 629 studying viral local adaptation. The genera belonging to each virus family are shown as well
 630 as the number of contigs and virus species within each virus family. Reference to the literature
 631 describing the detected family listed in the “reference” column [1–3].

Family	Genus	Contigs	Species	References
<i>Botourmiaviridae</i>		3	1	
	<i>Gammascleroulivirus</i>	3	1	
<i>Caulimoviridae</i>		896	21	[1,2,3]
	<i>Badnavirus</i>	1	1	
	<i>Caulimovirus</i>	842	15	
	<i>Soymovirus</i>	52	5	
<i>Closteroviridae</i>		13	5	[1,2,3]
	<i>Ampelovirus</i>	1	1	
	<i>Closterovirus</i>	11	3	
	unclassified	1	1	
<i>Partitiviridae</i>		212	11	[1,2,3]
	<i>Betapartitivirus</i>	113	8	
	unclassified	99	3	
<i>Pospiviridae</i>		24	1	[3]
	<i>Pospiviroid</i>	24	1	
<i>Tymoviridae</i>		3	1	[1,2,3]
	<i>Maculavirus</i>	3	1	

632

633

634

635

636 **Supplementary table 3.** Post hoc test comparing the infection status of the host *Plantago*
637 *lanceolata* from the three seed origin populations in a local adaptation experiment in the Åland
638 Islands during naturally occurring viral epidemics. Pairwise comparison of the estimated
639 marginal means calculated from both generalized linear mixed effects models A) model LF
640 and B) model HA (Table 1 and 2). P-values are Tukey adjusted.

A.

Contrast	Estimate	SE	Df	Z ratio	p-value
Seed origin population 876 – Seed origin population 950	1.283	0.703	Inf	1.825	0.161
Seed origin population 876- Seed origin population 9205	2.071	0.778	Inf	2.661	0.021
Seed origin population 950 – Seed origin population 9205	0.788	0.736	Inf	1.070	0.532

B.

Contrast	Estimate	SE	Df	Z ratio	p-value
Seed origin population 876 – Seed origin population 950	0.703	0.597	Inf	1.176	0.467
Seed origin population 876- Seed origin population 9205	1.818	0.649	Inf	2.802	0.014
Seed origin population 950 – Seed origin population 9205	1.115	0.664	Inf	1.679	0.213

641

642

643

644

645

646

647

648

649

650

651

652 **Supplementary table 4.** Model coefficients (model HA) testing for the effects of local
 653 adaptation on host infection status using the home *vs.* away metrics of local adaptation. For all
 654 variables one levels is a reference level included in the intercept.

Parameter	Coefficient	Std. Error	z-ratio	p-value
(Intercept)	0.46958	0.76237	0.61595	0.53792
Plant size	-0.00088	0.00067	-1.31035	0.19008
Seed origin population 950	-1.28293	0.70295	-1.82505	0.06799
Seed origin population 9205	-2.07082	0.77828	-2.66078	0.00780
Transplant population 950	-0.47045	0.67071	-0.70142	0.48304
Transplant population 9205	0.28314	0.59902	0.47267	0.63645
Seed origin population 876 \times sympatric	-0.86730	0.80862	-1.07257	0.28346
Seed origin population 950 \times sympatric	0.29316	0.83422	0.35141	0.72528
Seed origin population 9205 \times sympatric	-0.36200	0.92003	-0.39346	0.69398

655

656

657 Supplementary table 5. Explanatory and predictive performance of the HMSC model of viral
 658 occurrence in the experimental plant individuals in terms of Tjur R^2 and AUC. The model
 659 predictive performance is based on 10-fold cross-validation.

Response variable	Model explanatory performance		Model predictive performance with 10-fold cross validation (cv)	
	Tjur R^2	AUC	Tjur R^2 (cv)	AUC (cv)
<i>Caulimoviridae</i>	0.24	0.91	0.16	0.81
<i>Partitiviridae</i>	0.47	0.98	0.4	0.88
<i>Pospivirodæ</i>	0.1	0.8	0.01	0.54

660

661 **Supplementary table 6.** Exact values of the HMSC model variance partitioning for the three
662 most prevalent virus families detected in a reciprocal transplant experiment studying local
663 adaptation. Six variables explaining the virus family occurrence in a reciprocal transplant
664 experiment were: maternal line ID, seed origin population ID, sympatry/allopatry, plant size,
665 herbivory and transplant population ID (random).

666

Model parameter	Response variable		
Fixed effects:	<i>Caulimoviridae</i>	<i>Partitiviridae</i>	<i>Pospivirodae</i>
Maternal line	0.54	0.60	0.73
Seed origin population	0.35	0.33	0.18
Sympatry/allopatry	0.03	0.02	0.02
Plant area	0.07	0.03	0.03
Herbivory	0	0	0
Random effect:			
Transplant population	0.02	0.02	0.04

667

668

669

670

671

672

673 **References**

674

675 1. Hammond J. 1982 Plantago as a host of economically important viruses. *Adv. Virus Res.*
676 **27**, 103–140. (doi:10.1016/S0065-3527(08)60434-0)

677 2. Susi H, Filloux D, Frilander MJ, Roumagnac P, Laine AL. 2019 Diverse and variable
678 virus communities in wild plant populations revealed by metagenomic tools. *PeerJ*
679 **2019**. (doi:10.7717/peerj.6140)

680 3. Norberg A, Susi H, Sallinen S, Baran P, Clark NJ, Laine AL. 2023 Direct and indirect
681 viral associations predict coexistence in wild plant virus communities. *Curr. Biol.* **33**,
682 1665-1676.e4. (doi:10.1016/J.CUB.2023.03.022)

683

684